Tikrit Journal of Engineering Sciences (2024); 31(4): 92-101
DOI: http://doi.org/10.25130/tjes.31.4.9

IRAQI Academic Scientific Journals

ISSN: 1813-162X (Print); 2312-7589 (Online)
Tikrit Journal of Engineering Sciences
available online at: http://www.tj-es.com

TJES Tikrit Journal of Engineering Sciences

Design of an Axisymmetric Triangular Heatsink with Radial Arrangement: An Experimental Investigation of Natural Convection Heat Transfer

Jamal Bakr Khaleel [a], *Merdin Danışmaz* [a], *Tahseen Ahmad Tahseen* [b*], *Mohammed I. A. Tahseen* [c], *Thamer Khalif Salem* [d]

a Department of Mechanical Engineering, Kırşehir Ahi Evran University, Turkey.
b Mechanical Engineering Department, College of Engineering, University of Kirkuk, Kirkuk, Iraq.
c Mathematical Department, College of Education for Pure Sciences, Tikrit University, Tikrit, Iraq.
d Mechanical Engineering Department, College of Engineering, Tikrit University, Tikrit, Iraq.

Keywords:
Natural convection; Axisymmetric triangular heatsink; Vertical cylinder; Thermal resistance; Fins number.

Highlights:

- *Three heat sink models, I, II, and III, were investigated in the present study.*
- *An experimental investigation was conducted with an axisymmetric triangular radial heat sink.*
- *The best thermal resistance was in case III at the maximum Rayleigh number value.*

ARTICLE INFO

Article history:

Received	27 Sep.	2023
Received in revised form	01 Dec.	2023
Accepted	12 Dec.	2023
Final Proofreading	04 July	2024
Available online	11 Dec.	2024

Citation: Khaleel JB, Danışmaz M, Tahseen TA, Tahseen MIA, Salem TK. **Design of an Axisymmetric Triangular Heatsink with Radial Arrangement: An Experimental Investigation of Natural Convection Heat Transfer**. *Tikrit Journal of Engineering Sciences* 2024; **31**(4): 92-101.
http://doi.org/10.25130/tjes.31.4.9

**Corresponding author:*

Tahseen Ahmad Tahseen
Mechanical Engineering Department, College of Engineering, University of Kirkuk, Kirkuk, Iraq.

Abstract: Radial heat sinks are often employed as heat transfer enhancers because they increase the heat transfer surface area. Novel shapes of fins are used to enhance thermal heat performance under free convection heat transfer. The present experimental study investigates a new-fin shape effect on the thermal behavior of a radial heat sink with a circular base. The objective is to select the best reference model by comparing the three heat sink models, I, II, and III. The study was conducted for the heat-supplied rates of 20.16, 66.03, 105.30, 157.62, and 196.08 W. The present results showed that the fin in case I configurations dissipated heat transfer up to 12.07% and 30% compared to cases II and III, respectively, at high Rayleigh numbers. The thermal resistance in case III reduced to 13.91% and 16.23% compared to case I and case II, respectively, at the maximum Rayleigh number value. Then, based on experimental data, a correlation was suggested to estimate the Nusselt number for free convection from radial heat sink with vertically oriented double triangular fins.

تصميم مبدد حراري ذو ترتيب شعاعي وزعانف مثلثة بمحور متماثل: دراسة تجريبية لانتقال الحرارة بالحمل الطبيعي

جمال بكر خليل [١]، ميردين دانيشماز [١]، تحسين احمد تحسين [٢]، محمد ابراهيم احمد تحسين [٣]، ثامر خلف سالم [٤]

[١] قسم الهندسة الميكانيكية/ جامعة كيرشهر آهي افران/ كيرشهر- تركيا.

[٢] قسم الهندسة الميكانيكية/ كلية الهندسة/ جامعة كركوك/ كركوك - العراق.

[٣] قسم الرياضيات/ كلية التربية للعلوم الصرفة / جامعة تكريت/ تكريت - العراق.

[٤] قسم الهندسة الميكانيكية/ كلية الهندسة/ جامعة تكريت/ تكريت - العراق.

الخلاصة

غالباً ما يتم استخدام المشتتات الحرارية الشعاعية كمعززات لانتقال الحرارة لأنها تزيد من مساحة سطح انتقال الحرارة. اشكال جديدة من الزعانف تستخدم لتحسين السلوك الحراري للمشتتات الحرارية تحت ظروف انتقال الحرارة بالحمل الحراري الطبيعي. في هذه الدراسة يُسلط الضوء على اجراء دراسة تجريبية لتأثير شكل الزعنفة الجديدة على الأداء الحراري للأسطوانة العمودية. تمت مقارنة ثلاثة نماذج مختلفة للمشتت الحراري من أجل اختيار النموذج المرجعي الجيد. أجريت الدراسة بمعدلات كمية الحرارة المضافة وهي ٢٠,١٦، ٦٦,٠٣، ١٠٥,٣٠، ١٥٧,٦٢، ١٩٦,٠٨ W. بينت نتائج هذه الدراسة ان الزعنفة في الحالة الأولى تبدد الحرارة بنسبة تصل إلى ١٢,٠٧٪ و٣٠٪ مقارنة بالحالة الثانية والحالة الثالثة، على التوالي عند عدد رالي العالي. انخفضت المقاومة الحرارية في الحالة الثالثة إلى ١٣,٩١٪ و١٦,٢٣٪ مقارنة بالحالة الأولى والحالة الثانية، على التوالي في القيمة القصوى لرقم رالي. وبالاعتماد على البيانات التجريبية، تم اقتراح ارتباط لتقدير عدد نسلت للحمل الحراري الحر من المشتت الحراري الشعاعي ذي الزعانف المثلثية المزدوجة ذات الاتجاه العمودي.

الكلمات الدالة: الحمل الحراري الحر، زعانف مثلثة بمحور متماثل، أسطوانة عمودية، المقاومة الحرارية، عدد الزعانف.

1.INTRODUCTION

Developing high-efficiency electrical devices has attracted attention due to depleting fossil fuels and increaseing global energy use. Furthermore, producing light uses approximately twenty percent of the world's energy. The light emitting diode (LED) lightings that provide improved efficiency, longer life, and smaller size have displaced the conventional lighting devices. Thermal management, one of the variables to increase the lifetime of lighting systems, has significantly increased due to the rapid development of lighting devices over the past few decades. To keep LEDs cool, heat sinks have been used. About one-fifth of the total input energy in LED light bulbs is accounted for the photoelectric conversion efficiency, with the remaining energy released as heat [1-3]. Since natural convection requires no additional equipment, it is suggested for cooling LED lighting [4-8]. The LED lights' lifespan will be reduced because improperly designed heat sinks will cause the LEDs to heat rapidly [9-13]. Additionally, LED lighting is used in locations variety, and the setup angle can vary depending on the purpose and application. One of the important parameters in free convection cooling of LED lighting is the installation angle. Therefore, it is essential to investigate how heat sink cooling performance differs based on how devices are installed regarding gravity. Mhamuad et al. [14] studied the heat transfer for perforated fins under natural convection with rectangular fins. The free convection on heat sinks with different aluminum alloys is numerically studied by Nazzal et al. [15]. Heat transfer by free convection has been the focus of many investigations aimed at cooling heat sink with radial fins. Furthermore, Martynenko and Khramtsov [13] and Raithby and Hollands [16] studies condense it. The triangular fins have received less focus than plate or pin fins, given fin geometries for radial heat sinks. To calculate the rate of heat transfer from square fins positioned vertically and attached to a horizontal tube, Sparrow and Bahrami [17] used the naphthalene sublimation technique and experimental investigation. The investigation included the plate spacing and cylinder diameter affecting the heat transfer coefficient. Kim and Kim [18] investigated the natural convection heat transfer from vertical cylinders with pin fins. Experiments with different cylinder wall temperatures were conducted to determine the influence of fin pitch angles and fin heights on the heat transfer rates from finned cylinders to the surrounding air. The findings demonstrated that compared to conventional vertical cylinders with plate fins, the vertical cylinders with branched pin fins exhibited a 20% reduced thermal resistance. A correlation between the estimated thermal resistance and the Nusselt number values was also considered. The difference between the correlation of the experimental and predicted data was less than 20%. Lee et al. [19] investigated the cooling of electronic devices using horizontal tubes with rectangular fins at natural convection heat transfer. Based on the measurement data, a correlation of the predicted Nusselt number was proposed. A comparison was performed between the optimal cooling results from tubes with inclined and radially oriented rectangular fins. According to the comparison data, the tube with inclined fins performed 6% higher in cooling than that with radial rectangular fins. Tahseen et al. [20] numerically studied the influence of significant fin geometric perimeters and the Reynolds number on the thermal performance of a fin-and-tube heat exchanger. With an increase in Reynolds number, the overall heat transfer rate increased. The rate of transfer of heat was

positively influenced by fin density. However, the necessary pumping power increased with fin density. A staggered arrangement of tubes results in higher pressure drops than in-line arrangements of tubes [21-23]. Therefore, the tube pitch dimension plays an important role in calculating the heat transfer coefficient for the tube heat exchanger. The pressure drop and heat transfer were strongly related [21]. From the above literature review, few investigations have been conducted on the thermal behavior of radial heat sinks compatible with typical commercial LED lights, In Fig. 1 present the radial heat sink with attached to double-triangle fins. The current article objectives to find the thermal performance of this system at various input heat flows, fin numbers, and different fin shapes.

2.EXPERIMENT APPROACH

The experiments were conducted in an experimental laboratory designed and developed for studying convection heat transfer. Free convection heat transfer study employed a standardized and calibrated experimental setup. This setup is illustrated in Fig. 2. The experimental setup consisted of an aluminum cylinder, a heat sink equipped with heating elements, a data acquisition device, and a finned heat sink. The base vertical cylinder was heated by five heating elements ranging in power from 50 W to 850 W. The experimental data were recorded at every temperature location by the data acquisition system. Figure 3 shows the photograph of the test rig. The 167 W/(m K) is thermal conductivity of aluminum alloy was used to build the cylinder base of heat sinks.

Table 1 Geometrical Fin Array Dimensions for the Investigated Cases.

	Heat sink		
	CASE I	CASE II	CASE III
H_f (mm)	210	210	210
L_f (mm)	105	105	105
S (mm)	15	35	55
t (mm)	3	3	3

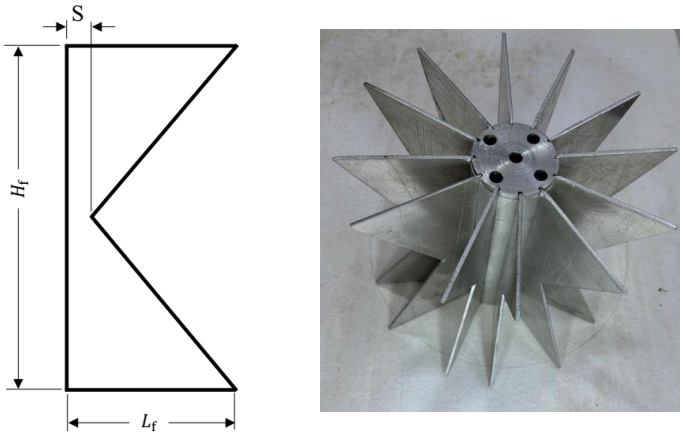

(a) Double triangle fins. **(b)** Heat sink photograph.

Fig. 1 The Base Cylinder with Fins.

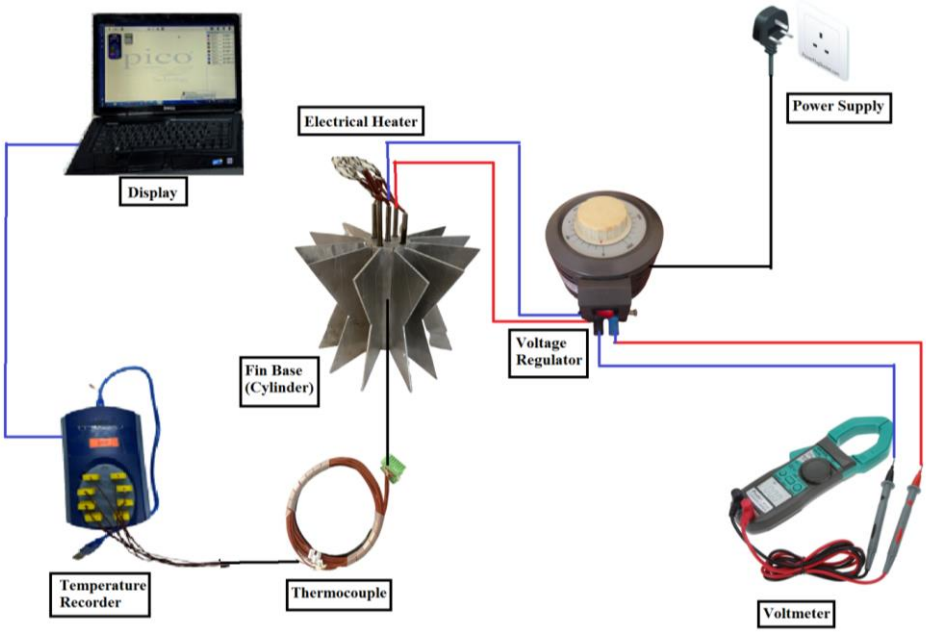

Fig. 2 Schematic of the Experimental Configuration.

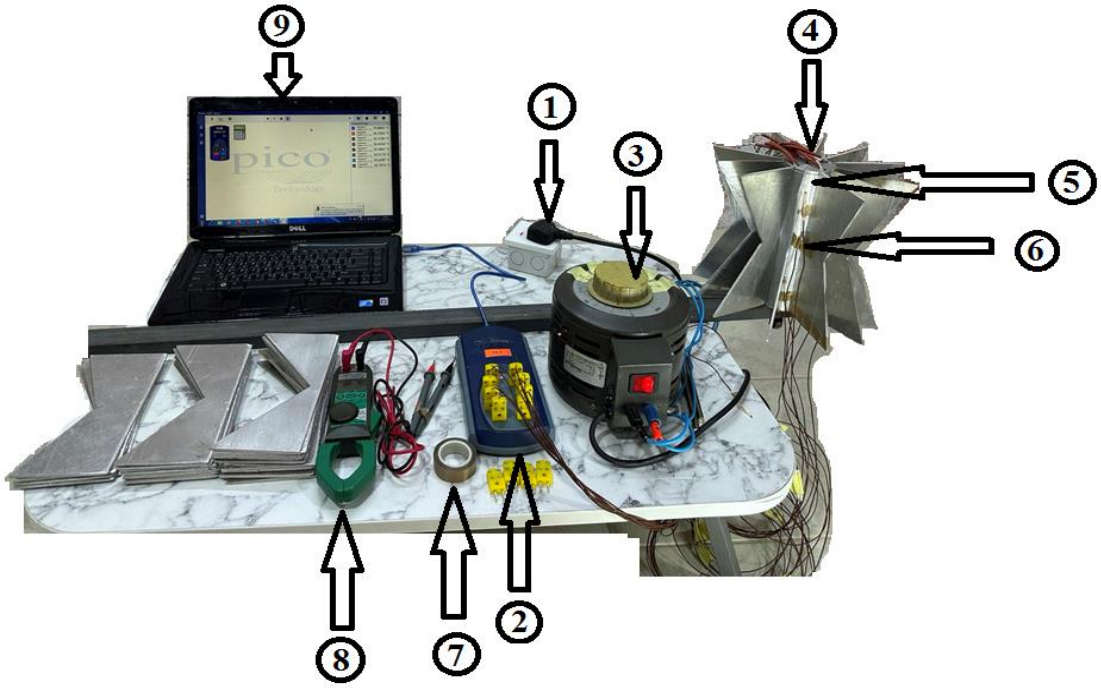

No.	Part Name	No.	Part Name	No.	Part Name
1	Electrical port	4	Cartridge heater	7	Tape
2	Data logger	5	Test rig	8	Voltage and current measurements
3	Power supply	6	Thermocouples	9	Laptop

Fig. 3 The Experimental Apparatus.

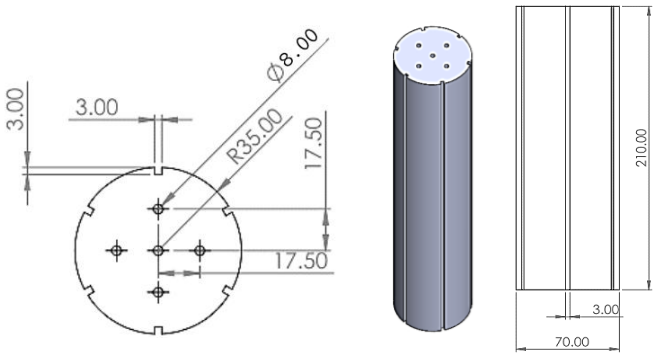

Fig. 4 Diagram of the Cylinder Cutaway (All Dimensions in mm).

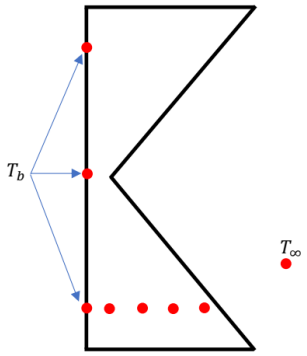

Fig. 5 Thermocouples Locations.

Nine heat sinks covered an extensive range of three cases and fin numbers. A solid aluminum cylinder was combined with double triangular fins made specifically for the experiments. Heat sinks were produced by overlapping bases and fins. The cylinders were 210 mm in length and 70 mm outside diameter. The base cylinder design with all dimensions is depicted in Fig. 4. Five holes of 8 mm in diameter and 200 mm in depth were drilled into the top of the cylinder. Double triangle fins with the twelve fins were setup in this investigation. Using a double triangle with upper and lower heights of 105 mm, a length the same as the cylinder with a 3 mm is thickness for each fin. The construction of the fins and the base cylinder are illustrated in Fig. 1. Table 1 presents the cases considered in the present study. The electric power source of the HSN 0103 model has an AC voltage range of 0-250 V and a maximum electric current of 5 A. The voltmeter used to measure the voltage had a voltage range of AC 2V to 750V. A clamp meter of the Pro'sKit MT-3102 type was used to measure the current, which maximum at 400 A. The resistors used in this study were cartridge heaters with a double step of 1000 Ω, which had a maximum dissipation of 50 W to 850 W at 220 V. To fit the installation of cast iron, electric resistors had a 200 mm length and a small (8 mm) outer diameter. Next, five cartridge heaters were inserted in the inner hole of the top cylinder base. The temperature was measured using eight calibrated K-type thermocouples. Four were fixed on the fin wall with three at the cylinder base. Outside the heat sink, another K-type thermocouple was used to measure the ambient temperature (see Fig. 5). The base temperature of these thermocouples was almost uniform in the vertical direction, with a maximum temperature difference of less

than 0.3 °C. Temperature data was collected utilizing a multichannel data acquisition. The Pico Technology USB TC-08 data acquisition model for thermocouple data loggers included an industrial temperature recorder with eight channels and an LCD (see Fig. 2). Each experiment was run three times. Uncertainty was examined to determine errors in the experimental results [24]. The experiments were conducted in a quiescent and isolated room. The radiation loss was evaluated and deducted from the total power supplied by the heater to estimate the net heat transfer rate from the heat sink. The details are as follows:

$$q_{\text{in}} = \Phi \times I \quad (1)$$

$$q_{\text{convection}} = q_{\text{in}} - q_{\text{radiation}} \quad (2)$$

$$Q_{\text{radiation}} = F\sigma A\varepsilon\left(T_b^4 - T_\infty^4\right) \quad (3)$$

It was estimated that less than 7% of the total heat was lost through the experimental investigation. The average temperature of the cylinder surface can be calculated by:

$$T_b = \frac{1}{3}\sum_{i=1}^{3} T_{b,\text{i}} \quad (4)$$

The heat flux can be written in the following form:

$$\dot{Q}_{\text{net}} = \frac{Q_{\text{convection}}}{A_b} \quad (5)$$

Where (A_b) is the cylinder base area and expressed as:

$$A_b = 2\left(\frac{\pi}{4}D^2\right) + \pi D H_{\text{f}} - N H_{\text{f}} t - 5\left(\frac{\pi}{4}d_{\text{heater}}^2\right) \quad (6)$$

Where (d_{heater}) is the electric heater diameter. The area of the fin from Fig. 2 can be estimated as follows:

$$A_{\text{fin}} = 2\left[H_{\text{f}} S - \frac{1}{2}(L_{\text{f}} - S)H_{\text{f}}\right] + \left[2L_{\text{f}} + 2 \times \sqrt{(H_{\text{f}}/2)^2 + (L_{\text{f}} - S)^2}\right] t \quad (7)$$

Therefore, the net heat transfer area with expression becomes:

$$A_{\text{net}} = A_b + N A_{\text{fin}} \quad (8)$$

The average free heat transfer coefficient can be estimated as follows [25]:

$$h = \frac{Q_{\text{net}}}{A_{\text{net}}(T_b - T_\infty)} \quad (9)$$

The Nusselt number (Nu) can be written as:

$$Nu = \frac{hH_{\text{f}}}{k_{\text{air}}} \quad (10)$$

Thus, the Rayleigh number (Ra) according to Eq. (11) is:

$$Ra = \frac{g\beta_{\text{air}}(T_b - T_\infty){H_{\text{f}}}^3}{\nu_{\text{air}}\alpha_{\text{air}}} \quad (11)$$

The heat sink thermal resistance is estimated using the experimental data as follows [11]:

$$R_{th} = \frac{(T_b - T_\infty)}{Q_{net}} \quad (12)$$

The present investigation focuses on the free stream outer layer. The engineering equation solver (EES) software was used to calculate the corresponding air properties. All properties used in Eqs. (10) and (11) were evaluated at the bulk temperature. To estimate the error in the experimental results, an uncertainty analysis was conducted. Accuracy and bias errors are included in the measurement error. The temperature measurement's accuracy error (Φ_T) is calculated using:

$$\Phi_T = t_{(N_{\text{data}}-1),95\%} \times \frac{\sigma_T}{\sqrt{N_{\text{data}}}} \quad (13)$$

Where $t95\%$, σ_T, and N_{data} data represent the t distribution with a 95% confidence level, the temperature's standard deviation, and data number and degree of freedom, respectively [26]. According to the manufacturer's statement, the bias error Ω_T is responsible for the instrument's inaccuracy in measuring temperature.

$$\Omega_T = 0.26℃$$

Uncertainty in the temperature measurement (Ψ_T) can be defined as:

$$\Psi_T = \pm\sqrt{{\Omega_T}^2 + {\Phi_T}^2} \quad (14)$$

Table 2 contains the estimated and presented temperature measurement Ψ_T uncertainty. The thermal resistance measurement ($\Psi_{R_{th}}$) uncertainty is defined as:

$$\frac{\Psi_{R_{th}}}{R_{th}} = \pm\sqrt{\left(\frac{\Psi_T}{T_b}\right)^2 + \left(\frac{\Psi_T}{T_\infty}\right)^2 + \left(\frac{\Psi_I}{I}\right)^2 + \left(\frac{\Psi_\phi}{\phi}\right)^2} \quad (15)$$

Where Ψ_I and Ψ_ϕ are the uncertainties in the current and voltage measurements. The investigation used thermocouples (0.03℃), a data acquisition instrument with a resolution of 0.1℃ and an accuracy of ±(0.2%+0.1)℃ to measure temperatures at each location.

Table 2 A Summary of Uncertainty Values.

Parameter	Uncertainty (%)
q_{in}	±6.33
Ra	±7.03
Nu	±4.46
R_{th}	±2.12

3.RESULTS AND DISCUSSION

The heat transfer characteristics of radial double triangle fins were examined in the present work. A selection of input heat rates, such as 20.16, 66.03, 105.30, 157.62, and 196.08 W with twelve fins, were tested during the experimental study. As indicated in the previous section, several studies were conducted on rectangular and triangle fins. In many engineering applications, the temperature distribution is a significant indicator of heat transfer [27]. As a result, in addition to the thermal resistance, the Nusselt number, the results of the present investigation were provided regarding the temperature distribution along the fin. The results were frequently displayed as graphs that illustrated the relationship between fin height, thermal resistance, Nusselt number and temperature distribution. The temperature distribution at the fin root was investigated in a several experiments. Figure 6 describes the variation of

the impact of height of fins on the difference temperature for various heat inputs with three cases tested. The temperature difference between cylinder surface and air temperatures is illustrated in Fig. 6. The temperature gradient increased with the heat input. On the other hand, the illustration's upper curve shows a decrease in temperature in the laminar flow region. The second curve displays a significant drop significantly distinguished from other curves because it is near the transitional region. The high heat input indicates a high-temperature difference. It is apparent that the temperature difference in case III is high because of the increased fin area. The thermocouples' locations at the fin surface (height of fin) are another important aspect examined in the present investigation. Figure 7 depicts the impact of fin height on base radial heat sink temperatures for various heat input rates in three cases. The figure compares the various surfaces to the ambient temperatures. As the fin height increased, temperatures decreased for all cases examined. If air was moving around and through the fin, the expected heating of the air at constant heat rates was pushed back. In this approach, the air and fin temperatures were kept sufficiently separated to optimize the fin's heat-removal performance.

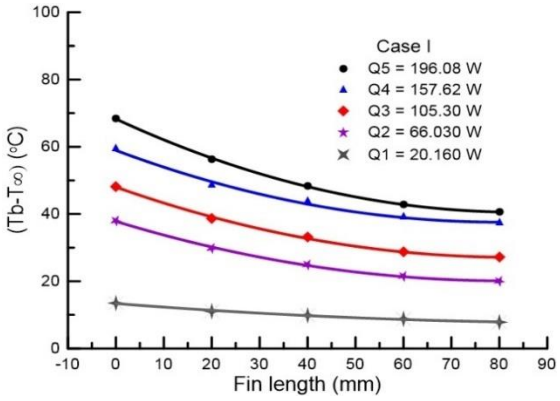

(a) Case I.

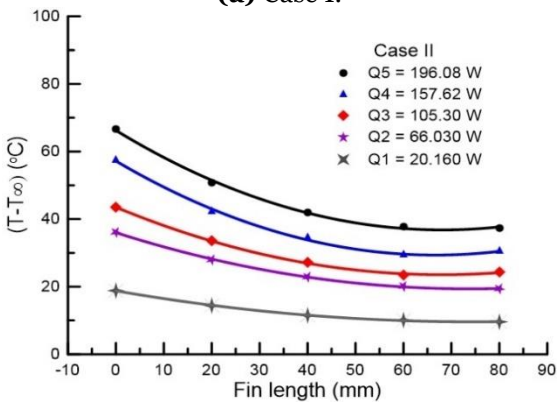

(b) Case II.

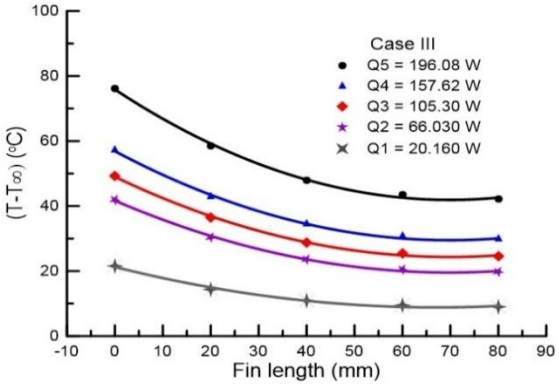

(c) case III.

Fig. 6 Temperature Profile for Different Fin Height and Heat Inputs at Three Cases.

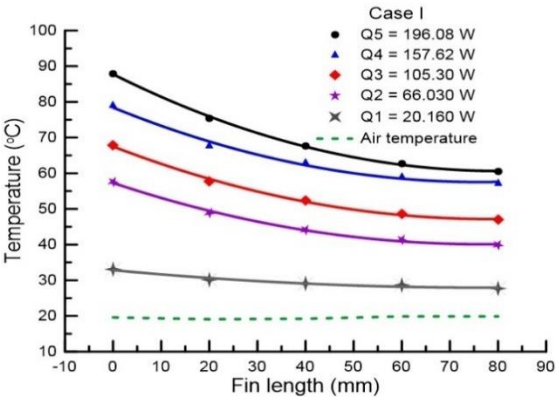

(a) Case I.

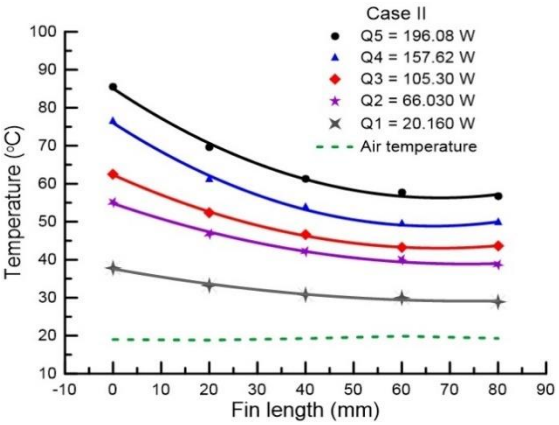

(b) Case II.

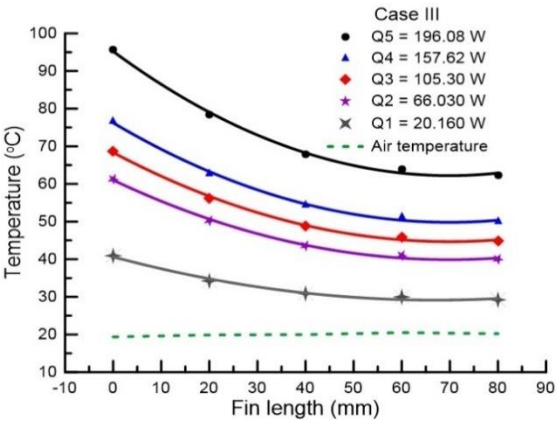

(c) Case III.

Fig. 7 The Effect of Fin Height on the Temperature Distribution in Three Cases Investigated.

Figure 8 shows the Nusselt number vs. Rayleigh number for three case studies. The Nusselt number increased in a non-linear trend with the Rayleigh number for all cases tested. Figure 8 clearly shows that using fins in case III decreased the Nusselt number compared with other cases. The maximum Nusselt number was in the heat sink in case I because the difference temperature between fin root and ambient decreased with fin surface area.

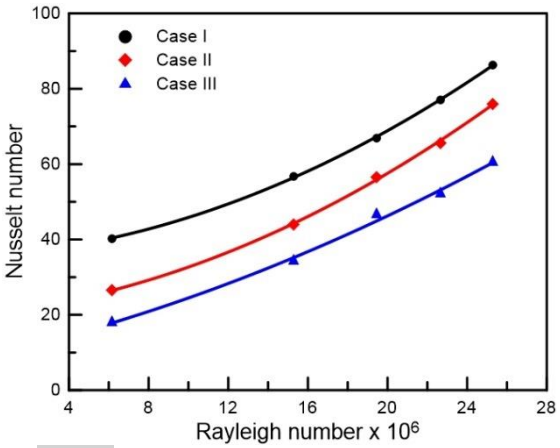

Fig. 8 Variation of the Heat Sink Nusselt Number as a Function of the Rayleigh Number in Different Cases.

Figure 9 provide the impacts of heat input on the thermal resistance in different studied cases. In every investigated case, the heat input increased lead to thermal resistance decreased. As the heat input increased, the thermal resistance decreased nonlinearly due to the fast fluid flow. A change in the fin enhanced the heat transfer rate and decreased the heat sink thermal resistance by increasing the effective heat transfer area due to the fin surface area increase.

Previous investigations yielded the functional form of the Nusselt number correlation, which was used to establish an acceptable correlation. The heat sink was cylinder-shaped and surrounded by both horizontal and vertical flows. Basically, the buoyancy force of the heated fluid produces a vertical flow that moves higher. To counterbalance the upward flow in

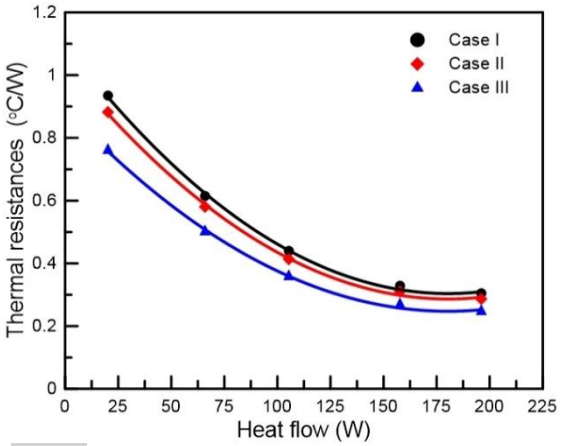

Fig. 9 Variation in Thermal Resistance Based on Heat Flow at Several Cases.

the inner region, the fluid entering from the surroundings provides an inward-moving horizontal flow. As a result, the overall flow pattern appears chimney-type and simulates a fin array over a horizontal surface. [11, 16, 28]. In the current study, such an initial approximation is obtained using the practical form of the Nusselt number correlation for the rectangular fin array on a horizontal surface. The Nusselt number correlation functional form, based on Harahap and McManus [28], is:

$$Nu = C\left(Ra\frac{A_{dir}}{H_f L_f}\right)^{n_1}\left(\frac{P_{ave}}{L_f}\right)^{n_2}\left(\frac{H_f}{L_f}\right)^{n_3}\left(\frac{S}{L_f}\right)^{n_4} \quad (16)$$

Where RaA_{dir}/H_fL_f, H_f/L_f, and P_{ave}/L_f denote the dimensionless fluid velocity, fin length, and fin-to-fin spacing, respectively. This correlation remained valid for a rectangular fin array on a horizontal surface within the range of $1.61 \times 10^7 < RaA_{dir}/H_fL_f < 6.62 \times 10^7$. The Rayleigh number ($Ra$), the cross-section area of airflow (A_{dir}), and average fin-to-fin spacing (P_{ave}) are represented in Eq. (16). The A_{dir} and P_{ave} are provided according to the radial heat sink with vertically doubled triangular fins case.

$$\left.\begin{aligned} A_{dir} &= \pi(D/2 + L_f)^2 - \pi(D/2)^2 \\ P_{ave} &= \pi(D + L_f)/N - t \end{aligned}\right\} \quad (17)$$

Using a least-squares fit, the empirical coefficients C, n_1, n_2, n_3, and n_4 that correspond to the Nusselt numbers computed from the experimental data are identified as:

$C = 10.18, n_1 = 0.772, n_2 = -48.772,$
$n_3 = -65.448, n_4 = -0.2772$
and

$$Nu = 10.18\left(Ra\frac{A_{dir}}{H_f L_f} \times 10^{-6}\right)^{0.772}\left(\frac{P_{ave}}{L_f}\right)^{-48.772}\left(\frac{H_f}{L_f}\right)^{-65.448}\left(\frac{S}{L_f}\right)^{-0.272} \quad (18)$$

Figure 10 (a) shows the result of Eq. (18). The maximum deviation was 7%, the average deviation was 4.8%, and the determination coefficient was $R^2 = 97.3\%$. The latter requirement is satisfied by Eq. (18), while the former condition is not applicable. As a result, in the present investigation, the correlation was modified as follows to satisfy both conditions [29]:

$$Nu = C\left(Ra\frac{A_{dir}}{H_f L_f} \times 10^{-6}\right)^{n_1}\left(\frac{P_{ave}}{L_f}\right)^{n_2}\left(\frac{H_f}{L_f}\right)^{n_3}\left(1 - \frac{S}{L_f}\right)^{n_4} \quad (19)$$

The least-square fitting method showed that the modified correlation was the closest to the Nusselt numbers obtained from the experimental data when the empirical coefficients were provided as:

$C = 1.227, n_1 = 0.771, n_2 = -0.01,$
$n_3 = 1.581, n_4 = 0.667$
Likewise

$$Nu_L = 1.227\left(Ra\frac{A_{dir}}{H_f L_f}\times 10^{-6}\right)^{0.771}\left(\frac{P_{ave}}{L_f}\right)^{-0.01}\left(\frac{H_f}{L_f}\right)^{1.581}\left(1-\frac{S}{L_f}\right)^{0.667} \quad (20)$$

Figure 10 (b) shows the result of Eq. (20). The maximum and mean deviations were 6.4% and 3.2%. The coefficient of determination was $R^2 = 99.1\%$. For another modified correlation for the closest to the Nusselt number according to Eq. (21):

$$Nu = C\left(Ra\frac{A_{dir}}{H_f L_f}\times 10^{-6}\right)^{n_1}\left[0.84+\frac{100}{n_2}\left(\frac{P_{ave}}{L_f}\right)^{n_3}\right]^{-1}\left(\frac{H_f}{L_f}\right)^{n_4}\left(1-\frac{S}{L_f}\right)^{n_5} \quad (21)$$

The empirical coefficients were given as,
$C = 4.043, n_1 = 0.771, n_2 = 2.835,$
$n_3 = 2.351, n_4 = 3.428, n_5 = 0.667$
The final Nusselt number correlation is:

$$Nu = 4.043\left(Ra\frac{A_{dir}}{H_f L_f}\right)^{0.771}\left[0.88+\frac{100}{2.835}\left(\frac{P_{ave}}{L_f}\right)^{2.351}\right]^{-1.5}\left(\frac{H_f}{L_f}\right)^{3.428}\left(1-\frac{S}{L_f}\right)^{0.667} \quad (22)$$

The result of Eq. (22), as presented in Fig. 10 (c), shows that the maximum and mean deviations are 5.7% and 3.1%. The coefficient of determination is $R^2 = 99.1\%$. In addition, these results indicate a good agreement between experimental data and predicted values.

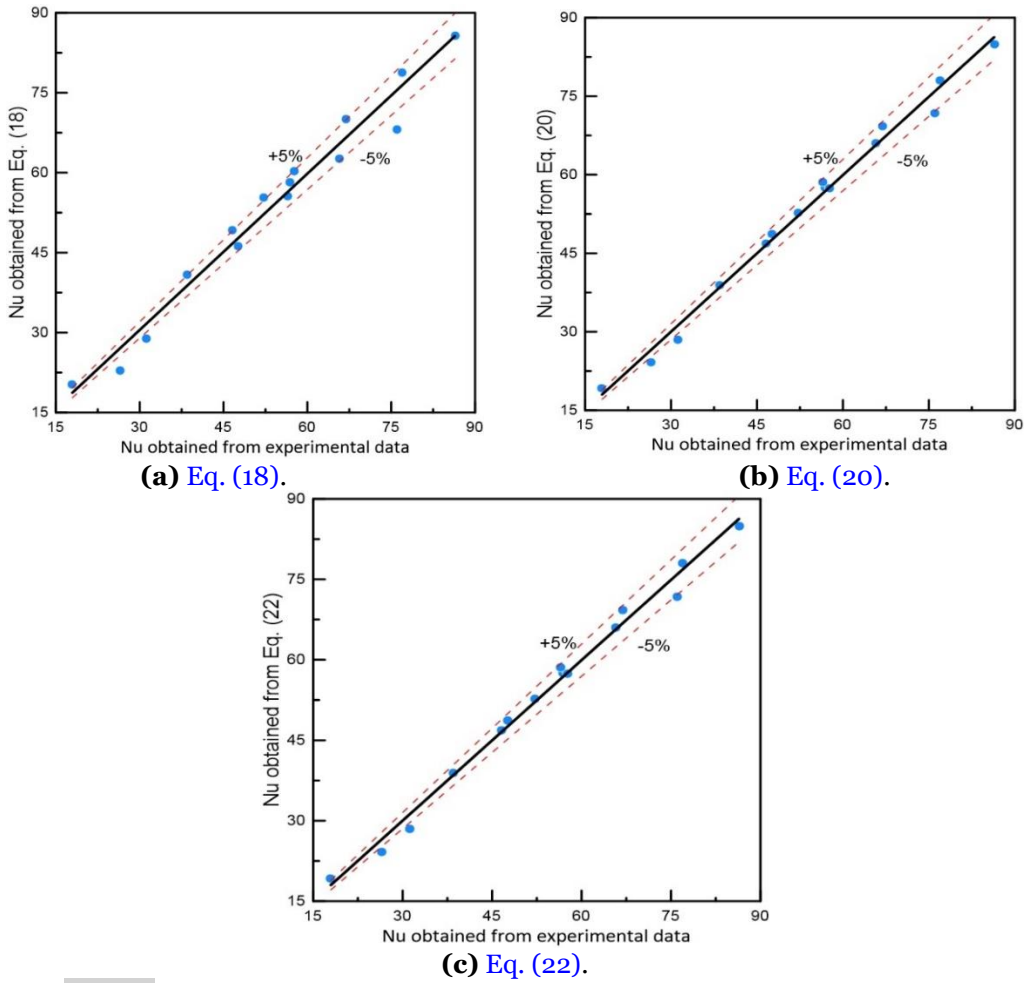

(a) Eq. (18). **(b)** Eq. (20).

(c) Eq. (22).

Fig. 10 Comparison between the Nusselt Numbers estimated from Modified Correlation and the Experimental Data.

4.CONCLUSION

A detailed analysis of free convection in radial heat sinks with radial double triangle fins was performed using three cases, i.e., I, II, and III, with five input heat rates at twelve fins. From the result, the Nusselt number increased with the Rayleigh number. In high Rayleigh numbers, the fin in case I configuration dissipated heat transfer more than case II and case III by 12.07% and 30%, respectively. The thermal resistance in case III was less than case I and case II by 13.91% and 16.23%, respectively, in maximum Rayleigh number. The Nusselt number developed correlation displayed good agreement with actual value (experimental) with an inaccuracy less than ±5% and coefficient of determination (R^2) up to 97%.

NOMENCLATURE

A	The area, m^2
Cp	Air heat capacity, J/(kg ℃)
D	Base cylinder diameter, m
g	Gravitational, m/s^2
h	Heat transfer coefficient, W/(m^2℃)
H_f	The fin length, m
I	The current, A
k	Thermal conductivity, W/(m ℃)
L_f	The fin height, m
N	The fins number
Nu	Nusselt number
Q	The heat input, W
Ra	Rayleigh number
R_{th}	The thermal resistance, ℃/W
t	The thickness of fin, m
T	Temperature, ℃
Greek symbols	
α	Thermal diffusivity, m^2/s
β	Expansion coefficient, 1/K
μ	Dynamic viscosity, kg/(m s)
ν	Kinematic viscosity, m^2/s
ρ	Density, kg/m^3
ε	Emissivity
Φ	The voltage input, V
Subscripts	
b	The fin root
in	The input
∞	ambient

REFERENCES

[1] Jang D, Yu S-H, Lee K-S. **Multidisciplinary Optimization of a Pin-Fin Radial Heat Sink for LED Lighting Applications**. *International Journal of Heat and Mass Transfer* 2012; **55**:515-521.

[2] Hussein YH, Akroot A, Tahseen TA. **Investigation of Free Convection Heat Transfer from Vertical Cylinders with Semicircular Fins.** *Experimental Heat Transfer* 2023:1-20.

[3] Kwak D-B, Noh J-H, Lee K-S, Yook S-J. **Cooling Performance of a Radial Heat Sink with Triangular Fins on a Circular Base at Various Installation Angles**. *International Journal of Thermal Sciences* 2017; **120**:377-385.

[4] Christensen A, Graham S. **Thermal Effects in Packaging High Power Light Emitting Diode Arrays**. *Applied Thermal Engineering* 2009; **29**:364-371.

[5] Shen Q, Sun D, Xu Y, Jin T, Zhao X, Zhang N, Wu K, Huang Z. **Natural Convection Heat Transfer Along Vertical Cylinder Heat Sinks with Longitudinal Fins**. *International Journal of Thermal Sciences* 2016; **100**:457-464.

[6] Huang G-J, Wong S-C, Lin C-P. **Enhancement of Natural Convection Heat Transfer from Horizontal Rectangular Fin Arrays with Perforations in Fin Base**. *International Journal of Thermal Sciences* 2014; **84**:164-174.

[7] Hassan MS, Tahseen TA, Weis MM. **Natural Convection from a Radial Heat Sink with Triangular Fins**. *NTU Journal of Engineering and Technology* 2022; **1**:40-49.

[8] Hassan MS, Weis MM, Tahseen TA. **Heat Transfer Around a Radial Heat Sink with Triangular Fins Cooled by Natural Convection**. *Design Engineering* 2021; **8**:16766-16784

[9] Chen L, Yang A, Xie Z, Sun F. **Constructal Entropy Generation Rate Minimization for Cylindrical Pin-Fin Heat Sinks**. *International Journal of Thermal Sciences* 2017; **111**:168-174.

[10] An BH, Kim HJ, Kim D-K. **Nusselt Number Correlation for Natural Convection from Vertical Cylinders with Vertically Oriented Plate Fins**. *Experimental Thermal and Fluid Science* 2012; **41**:59-66.

[11] Lee M, Kim HJ, Kim D-K. **Nusselt Number Correlation for Natural Convection from Vertical Cylinders with Triangular Fins**. *Applied Thermal Engineering* 2016; **93**:1238-1247.

[12] Lee G-W, Kim HJ, Kim D-K. **Experimental Study on Horizontal Cylinders with Triangular Fins under Natural Convection**. *Energies* 2018; **11**:836(1-15).

[13] Martynenko OG, Khramtsov PP. ***Free-Convective Heat Transfer***. New York, USA: Springer, 2005.

[14] Mhamuad AM, Ibrahim TK, Jasim RR. **Determination of the Temperature Distribution the Perforated Fins Under Natural Convection**. *Tikrit Journal of Engineering Sciences* 2008; **15**(2):63-78.

[15] Nazzal IT, Salem TK, Farhan SS, Tahseen. **Investigation into the Heat Sink Performance of the Inline and Cut Cross Fins Types Using Different Aluminum Alloys**. *Journal of Thermal Engineering* 2024; **10**(1):10-20.

[16] Raithby GD, Hollands KGT. ***Natural Convection***. In: Rohsenow WM, Hartnett JP, Cho YI, (Eds.), Handbook of Heat Transfer. New York, USA: McGraw-Hill, 1998. Chapter 4; pp. 220-318.

[17] Sparrow E, Bahrami P. **Experiments on Natural Convection Heat Transfer on the Fins of a Finned Horizontal Tube**. *International Journal of Heat and Mass Transfer* 1980; **23**(11):1555-1560.

[18] Kim D, Kim DK. **Experimental Study of Natural Convection from Vertical Cylinders with Branched Pin Fins**. *International Journal of Heat and Mass Transfer* 2021; **177**: 121545(1-10).

[19] Lee JB, Kim HJ, Kim D-K. **Thermal Optimization of Horizontal Tubes with Tilted Rectangular Fins under Free Convection for the Cooling of Electronic Devices**. *Applied Sciences* 2017; **7**(4): 352(1-15).

[20] Tahseen TA, Rahman M, Ishak M. **Effect of Tube Spacing, Fin Density and Reynolds Number on Overall Heat Transfer Rate for In-Line Configuration**. *International Journal of Automotive & Mechanical Engineering* 2015; **12**: 3065-3075.

[21] Tahseen TA, Ishak M, Rahman M. **An Overview on Thermal and Fluid Flow Characteristics in a Plain Plate Finned and Un-Finned Tube Banks Heat Exchanger**. *Renewable and Sustainable Energy Reviews* 2015; **43**: 363-380.

[22] Jassim AH, Rahman M, Hamada KI, Ishak M, Tahseen TA. **Hybrid CFD-ANN Scheme for Air Flow and Heat Transfer across in-Line Flat Tubes Array**. *Tikrit Journal of Engineering Sciences* 2018; **25**(2):59-67.

[23] Jassim AH, Tahseen TA, Mustafa AW, Rahman MM, Ishak M. An **Experimental Investigation in Forced Convective Heat Transfer and Friction Factor of Air Flow Over Aligned Round and Flattened Tube Banks**. *Heat Transfer-Asian Research* 2019; **48**: 2350-2369.

[24] Figliola RS, Beasley DE. ***Theory and Design for Mechanical Measurements*** (Fifth ed.) New Youk, USA: John Wiley & Sons, Inc., 2011.

[25] Bergman TL, Lavine AS, Incropera FP, Dewitt DP. ***Introduction to Heat Transfer.*** (Sixth ed.) New York, USA: John Wiley & Sons., 2011.

[26] Holman JP. **Experimental Methods for Engineers.** (Eighth ed.) New York, USA: McGraw-Hill., 2021.

[27] Kraus AD, Aziz A, Welty J, Sekulic D. **Extended Surface Heat Transfer**. *Applied Mechanics Reviews, AEME* 2001 **54**(5):B92(102-160).

[28] Harahap F, McManus HN. **Natural Convection Heat Transfer from Horizontal Rectangular Fin Arrays**. *Journal of Heat Transfer* 1967; **89**:32-38.

[29] Yu S-H, Lee K-S, Yook S-J. **Natural Convection around a Radial Heat Sink**. *International Journal of Heat and Mass Transfer* 2010; **53**(13-14):2935-2938.